THE MODELING OF FUEL ROD BEHAVIOUR UNDER RIA CONDITIONS IN THE CODE DYN3D

Ulrich Rohde

1. Introduction

The code DYN3D has been developed in the Research Centre Rossendorf for the analysis of reactivity initiated accidents (RIA) in light water reactors [1]. It comprises 3D neutron kinetics based on a nodal expansion approach both for hexagonal and square fuel element geometry and a thermo-hydraulic model of the reactor core. In RIA analysis, the heat transfer from fuel to coolant plays an important role. This heat transfer is significantly affected by the behaviour of the gas gap between fuel and cladding, but also by the heat transfer conditions at the cladding surface. Therefore, a transient fuel rod behaviour model is implemented into DYN3D [2,3]. This model is coupled with a heat transfer regime map for cladding surface - coolant heat transfer ranging from subcooled liquid convection conditions to dispersed flow with superheated steam. For the validation of the model, experiments on fuel rod behaviour during RIAs carried out in Russian and Japanese pulsed research reactors are calculated. Because the experiments were carried out under atmospheric pressure and stagnant flow conditions, additional calculational studies on the fuel rod behaviour during RIAs in power reactors at high pressure and high mass flow rate conditions were performed.

2. Fuel Rod Model

For the estimation of fuel and cladding temperatures the heat conduction equation in one–dimensional radial geometry is solved numerically taking into account temperature–dependent heat conductivity. However, the main problem of fuel rod behaviour modelling is the determination of heat transfer coefficients α_{gap} at the gas gap between fuel and cladding and α_c from cladding to coolant.

The general idea of the gas gap behaviour modeling in DYN3D is that the parameters for the stationary reference state (e.g. geometrical gap width, gas pressure and composition) are known from detailed fuel rod behaviour codes. The changes of the gas gap parameters during the transient process due to variation of gap width, gas temperature and pressure, coolant and fuel - cladding contact pressure are estimated by the DYN3D model.

In the gas gap between fuel and cladding the heat transfer components due to conduction in the gas, radiation and fuel–cladding contact are considered. The heat transfer coefficient due to conduction in the gas is determined by

$$\alpha_{cond} = \frac{\lambda_{g,\,mix}}{\delta_{gap} + \delta_{roug} + \delta_{ext}} \qquad (1)$$

where $\lambda_{g,mix}$ is the thermal conductivity of the filling gas mixture. The composition of the filling gas mixture is a function of the actual depletion state and must be obtained from detailed fuel rod behaviour codes. δ_{gap} is the geometrical gap width and is determined by using a thermo-mechanical model. δ_{roug} is related to the surface roughness values of fuel and cladding. δ_{ext} is a gas kinetics extrapolation length. The radiation component α_{rad} is given by the Stefan–Boltzmann law. In the case of closed gap, heat transfer due to contact conductance is considered:

$$\alpha_{cont} = \frac{C\lambda_{f,c}}{\delta_{sr}^{n}}\left(\frac{p_{cont}}{H}\right)^{m} \quad (2)$$

where C, m and n are constants, δ_{sr} is the square averaged surface roughness, p_{cont} the contact pressure, H the Meyer hardness of the softer material (fuel or cladding), $\lambda_{f,c}$ is the effective thermal conductivity at the fuel-cladding interface.

The contact pressure is estimated based on the following assumptions:
– one–dimensional modeling of mechanics in radial direction,
– linear superposition of radial thermal, elastic and plastic deformations without axial coupling,
– elastic deformation of the fuel is taken into account only in the case of fuel–cladding contact, plastic deformations of the fuel are not considered,
– cladding is described in the thin shell approximation.

The cladding stress is determined by the gas pressure inside the cladding, the outer coolant pressure and, possibly, the contact pressure. The gas pressure p_{gas} is obtained from the ideal gas law for the filling gas and taking into account the change of gas temperature as well as the change of free volume by changing gas gap width.

The plastic deformation of the cladding is considered in accordance with the creeping law:

$$\varepsilon = \frac{\delta R}{R} = \left(\frac{\sigma}{K\dot{\varepsilon}^{q}}\right)^{1/p} \quad (3)$$

where the coefficients K, p and q are material properties. $\dot{\varepsilon}$ is the strain rate, that means, the time-derivative of the cladding strain $\varepsilon = \delta R/R$. Plastic deformation is considered, when the stress exceeds the yield strength $\sigma_{yield,}$ which is a material property and a function of temperature and strain rate.

If the pressure outside the cladding is larger than the inner pressure, prompt creeping of the cladding on the fuel is assumed so that the gap vanishes and the cladding stress is zero. If the inner pressure exceeds outer pressure, two different situations are considered. If the gap is closed and the contact pressure is non-zero, it is assumed that prompt creeping will take place reducing the stress until it becomes equal to the yield strength. If there is no fuel - cladding contact and the gas pressure exceeds the coolant pressure, time-dependent creeping will be considered according to equation (3). The last situation is typical for low coolant pressures like in RIA experiments at pulsed research reactors or in LOCA cases and leads to cladding ballooning, while the first one is typical for RIA conditions in power reactors.

A mechanistic model of fuel rod failure during accidents is not included in DYN3D, but some parameters needed for the assessment of fuel rod integrity are provided:
- fuel enthalpy for each axial node of the rod,
- cladding oxide thickness,
- signalization of possible cladding rupture, when the cladding stress is positive (inner pressure is larger than outer pressure) and exceeds the yield strength.

The cladding oxidation due to metal-water reactrion (MWR) at high temperatures is described by the equation:

$$D\frac{dD}{dt} = \frac{A}{C^{2}}\exp\left(\frac{-B}{T}\right) \quad (4)$$

where D is the oxide layer thickness , T the cladding surface temperature, C the mass density of oxygen in ZrO_2 , A and B are constants. The MWR is considered as an additional heat source in the cladding, but the additional heat transfer resistance at the cladding surface and the change of mechanical properties of the cladding caused by the oxide layer are not taken into account (restriction to thin oxide layers).

3. Heat Transfer Regime Map

The heat transfer from fuel to coolant, and in this way the fuel rod behaviour, is affected not only by the behaviour of the gas gap, but also by heat transfer conditions at the cladding surface,. In DYN3D, a heat transfer regime map is used which covers all flow regimes from one-phase liquid convection over different boiling heat transfer mechanisms to superheated steam convection.

Appropriate correlations for single phase convection and the region of boiling heat transfer are chosen from [4]. The occurence of heat transfer crisis is determined from various critical heat flux correlations . For low mass flow densities ($G << 200$ kg/m^{2}s) the Kutateladse correlation for $q"_{crit}$ with a non-equilibrium correction is used [4]. An additional criterion for the detection of dryout is considered. After reaching the critical heat flux or critical dryout quality, the heat transfer is decreasing, which leads to an increasing temperature difference between the heated wall and the fluid. In this unstable transition boiling region the heat flux is interpolated between the critical heat flux value and the value at the minimum stable film boiling point. In the stable post-crisis region heat transfer correlations for inverted annular or dispersed flow are used. Additionally, the heat transfer from wall to coolant by radiation is taken into account. After full evaporation of coolant, heat transfer to superheated steam is estimated by a single phase forced convection correlation .

The following additional non-equilibrium corrections due to subcooled liquid are applied to the Leidenfrost or minimum stable film boiling point T_{MSFB} and the heat transfer coefficients in the post crisis region :

$$T_{MSFB} = T_{sat} + 350 + 5.1\,(T_{sat} - T_{liq}) \tag{5}$$

$$\alpha_{pc}(T=T_{liq}) = \alpha_{pc}(T=T_{sat})[1 + 0.025\,(T_{sat} - T_{liq})] \tag{6}$$

The formulaes (5) and (6) are based on correlations proposed by Ohnishi et al. [8].

4. Calculations for RIA Experiments

For the validation of the fuel rod and heat transfer model in the code DYN3D several experiments from literature were calculated. Experiments on the fuel behaviour during large power pulses were carried out e. g. in the Japanese Nuclear Safety Research Reactor (NSRR) reported about in [6], in the Russian research reactors IGR and GIDRA [7] and in the frame of the French CABRI experimental program [5]. The NSRR is a modified TRIGA reactor whith a power pulse half width of a few milliseconds. The Russian GIDRA reactor contains an aqueous solution of enriched fuel producing narrow power pulses, while the IGR recator is a graphite moderated one with higher pulse half - width between 0,5s and a few seconds. Experimental results of tests where shortened probes of fresh fuel rods were inserted into a water or air filled capsule are provided in [8], [9] and [10]. In all tests, the water was at atmospheric pressure. An overview of the

experiments calculated by use of the DYN3D fuel rod model is given in Table 1.

Table 1: Overview on RIA experiments calculated with the DYN3D fuel rod model - experimental and calculated results

		NSRR Experiments			IGR Experiments				
Exp. Nr.		1	2	3	4	5	6	7	8
ΔE [cal/g]		190	190	190	207	284	326	360	93
τ [ms]		7	7	7	1050	650	500	800	4300
ΔT [K]		10	40	80	80	80	80	80	Air
$h_{f,max}$ [cal/g]		187	185.5	183.5	123	179	216	200	-
T_{clad} [^oC]	meas.	1500	1330	1000	141	177	967	940	1200
	calc.	1447	1278	1177	153	167	891	1040	1320
t_{rewet} [s]	meas.	38	15	10	-	-	6.3	11.0	-
	calc.	41	20	7.2	-	-	6.6	12.5	-
δ_{OX} [μm]	meas.	12	8	5	-	-	-	-	-
	calc.	29	13	7	-	-	-	-	-

ΔE is the energy release in the fuel probe, τ - the power pulse half-width, ΔT - the coolant subcooling, $h_{f,max}$ - the energy deposition in the fuel (calculated), T_{clad} - the maximum cladding temperature, t_{rewet} - the time until rewetting after heat transfer crisis, δ_{OX} - the oxide layer thickness due to cladding oxidation.

In general, a good agreement is achieved between the calculations and the experiments, which were performed in very different conditions (pulse half width, coolant subcooling, energy release).The comparison between calculated and measured cladding temperatures for the IGR experiment No. 6 (see the table) is shown in fig. 1, for the NSRR experiments (number 1, 2 and 3) in fig. 2.

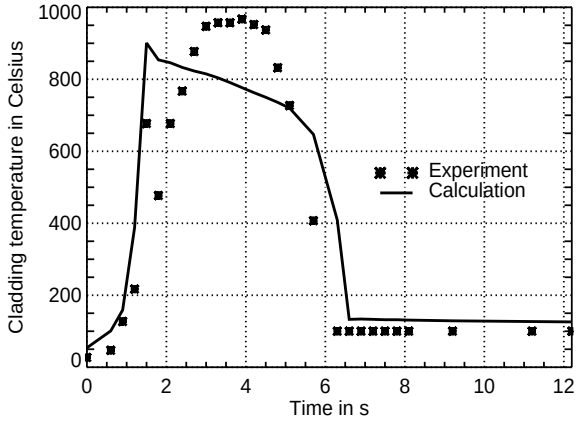

Fig. 1: Comparison for IGR RIA experiment Nr.6

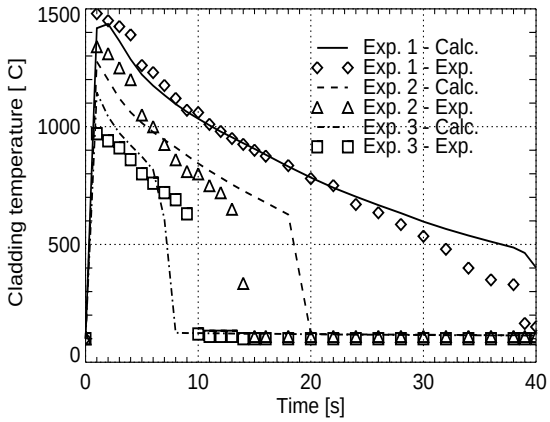

Fig. 2: Measurement and calculation for the NSRR RIA experiments

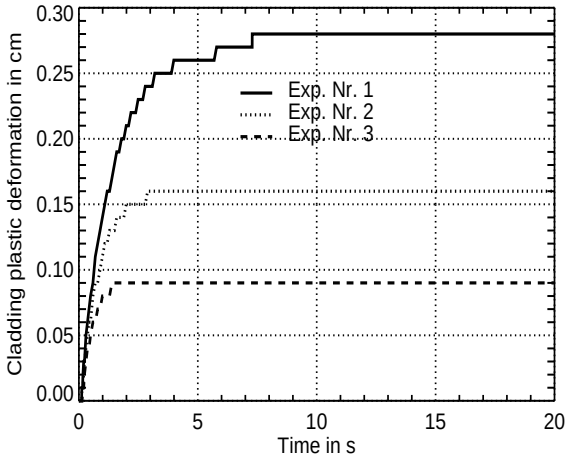

Fig. 3: Calculated cladding plastic deformation

The behaviour of the cladding and fuel temperature is very sensitive to the gas gap behaviour. In the first milliseconds, the gap is closed due to thermal expansion of the fuel. This increases the heat transfer from fuel to cladding and leads to very fast cladding heating. The cladding material becomes plastic and the cladding starts to expand. The calculated plastic deformation of the cladding (increase of cladding radius) for the NSRR experiments is shown on fig. 3. Experimental data on the cladding ballooning in these experiments are not available. Fig. 4 shows the cladding stress and yield strength of the cladding material. Within the first tenth of second, the yield strength is decreasing very rapidly due to the rising cladding temperature. When the stress becomes equal to the yield strenght, the plastic deformation of the cladding starts (see left part of fig. 4). After decrease of the cladding temperature due to the decreased heat transfer from fuel to cladding, the yield strength is increasing and the plastic deformation stops (see right part of fig. 4 and fig. 3). If the plastic deformation would have not been taken into account, much higher cladding temperatures would be obtained.

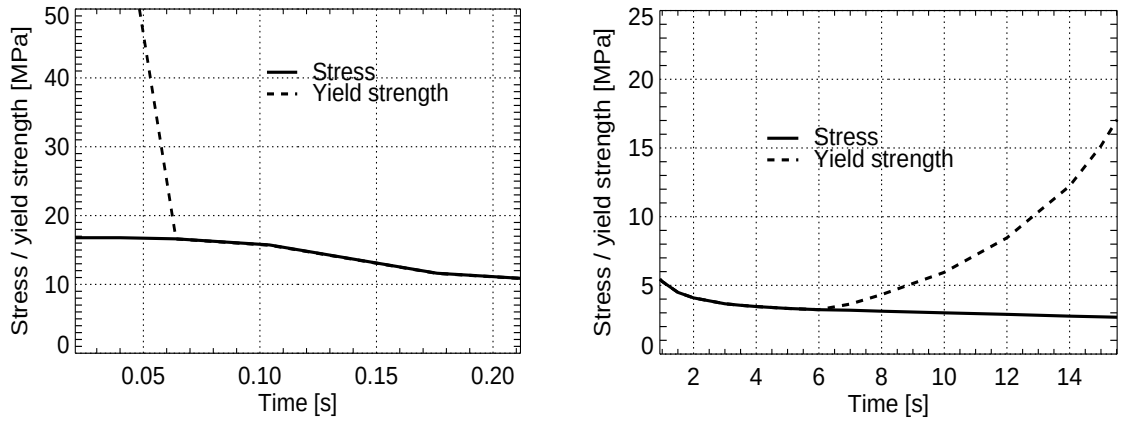

Fig. 4: Calculated stress and yield strength of the cladding for Exp. No. 1

Remarkable differences can be seen between the NSRR and the IGR experiments. In the NSRR experiments, the energy release in the burst was lower than in the IGR experiments with water cooling, but much higher cladding temperatures are reached. This is due to the very small pulse width which leads to an almost adiabatic heating of the fuel rod during the burst. In the NSRR experiments considered, the effect of coolant subcooling was investigated while the other conditions (energy release, pulse width) were fixed. This allows to adjust the heat transfer model.

However, the experiments were carried out under atmospheric pressure and stagnant flow conditions, while for RIAs in power reactors high pressure and high flow rate conditions are typical. Additional calculational studies on the fuel rod behaviour under power reactor conditions were performed, where reactor power peak curves with a half-width of 0.4 s and different energy release values were given as input to the fuel rod model calculations. Burn-up dependent data for the nominal state of the gas gap were obtained from calculations with the code STOFFEL [11].

In comparison with the experimental data from the research reactors, for the same energy deposition in the fuel and about the same pulse half-width, higher cladding temperatures are reached under power reactor conditions. This is due to the different gap behaviour. While at low coolant pressure the ballooning effect is observed, at higher pressures the cladding creepes on the fuel. The gap is closed and the heat transfer from fuel to cladding is enhanced.

The calculations have shown that the relevant mechanism of fresh fuel failure is melting, the fuel enthalpy at failure is about 230 cal/g. For burned-up fuel, cladding failure is possible due to high mechanical stress at much lower fuel enthalpy values (about 125 cal/g for a burn-up of 25 MWd/kg). This corresponds to results reported about in [12].

5. Conclusions

For the validation of the transient fuel rod model used in DYN3D, experiments on fuel rod behaviour during RIAs carried out in Russian and Japanese pulsed research reactors with shortened probes of fresh fuel rods are calculated. A good agreement between calculated and measured results was achieved.

Numerical studies concerning the fuel rod behaviour under RIA conditions in power reactors demonstrated, that the fuel rod behaviour at high pressures and flow rates in power reactors is different from the behaviour under atmospheric pressure and stagnant flow conditions in the experiments. The mechanisms of fuel rod failure for fresh and burned fuel reported from the literature can be qualitatively reproduced by the DYN3D model. However, the model must be extended and improved for proper description of burned fuel behaviour.

References

[1] U. Grundmann and U. Rohde (1996), DYN3D - a 3-dimensional Core Model for Steady-state and Transient Analyses of Thermal Reactors, Proc. Int. Conf. on the Physics of Reactors PHYSOR 96, Mito (Japan), pp. J-70 - J-79

[2] U. Rohde (1992), Modeling of Fuel Rod Behaviour and Heat Transfer in the Code FLOCAL for Reactivity Accident Analysis of Reactor Cores, in: Recent Advances in Heat Transfer, Elsevier Publ., Amsterdam, 1992

[3] U. Rohde: The Modeling of Fuel Rod Behaviour under RIA Conditions in the Code DYN3D, Annals of Nuclear Energy, to be published

[4] L.N. Poljanin, M. Ch. Ibragimov, G. P. Sabeljev (1982), Teploobmen v jadernykh reatorakh, Moscow, Ehnergoatomizdat

[5] Papin, J. et al. (1996), Nuclear Safety 37, 289 - 327

[6] T. Fuketa et al. (1996), Nuclear Safety **37**, 328 - 342

[7] V. Asmolov and L. Yegorova (1996), Nuclear Safety **37**, 343 - 352

[8] N. Ohnishi, K. Ishijima and S. Tanzawa (1984), Nucl. Sc. and Engineering **88**, 331-341

[9] V. Asmolov et al. (1987), Kernenergie **30**, 299-304

[10] E. Burmistrov, S. Bashkirzev and U. Rohde (1993), Validation Experience for FLOCAL, ESCES, MAIVA, SCDAP/RELAP Codes on the Basis of Post-Test Calculations for Russian and Japanese RIA Experiments“, Internal Report, Research Centre Rossendorf

[11] D. Reinfried (1985), Zur mathematischen Modellierung des Bestrahlungsverhaltens von Druckwasserreaktorbrennstäben, PhD Thesis, Rossendorf

[12] E. L. Courtright (1979), A Survey of Potential Light Water Reactor Fuel Rod Failure Mechanisms and Damage Limits, *N*UREG/CR - 1132 (PNL - 2787), 1979